Swiss Journal of Geosciences (2018) 111:191–204
https://doi.org/10.1007/s00015-017-0290-3

Knickpoints along the upper Indus River, Pakistan: an exploratory survey of geomorphic processes

Muhammad F. Ahmed[1] · J. David Rogers[2] · Elamin H. Ismail[2]

Received: 7 January 2017 / Accepted: 13 December 2017 / Published online: 16 January 2018
© Swiss Geological Society 2017

Abstract
This article summarizes an exploratory study carried out to investigate the significance of various geomorphic features on the formation of observed knickpoints along the upper Indus River in northern Pakistan. These features include bedrock lithology, active faults, sediment flux from tributary channels, and landslide dams which have blocked the main channel. The knickpoints and their related geomorphic parameters (channel profile, concavity, drainage area and normalized steepness index, etc.) were extracted from Advanced Spaceborne Thermal Emission and Reflection (ASTER) Global Digital Elevation Models (GDEMs) with 30 m resolution using ArcGIS, River Tools, and Matlab software. A total of 251 major and minor knickpoints were extracted from the longitudinal profile along a ~ 750 km reach upstream of Tarbela Reservoir. The identified knickpoints and their respective normalized steepness index (k_{sn} values) were compared with bedrock lithology, mapped faults, regional landslide/rockslide inventory, and the locations of historic landslide dams. The analyses revealed that the knickpoints do not correlate with the bedrock lithology except where major unit boundaries coexist with mapped faults, especially in reaches criss-crossed by active thrust faults in the Nanga Parbat Haramosh (NPHM) region. Neither did the river's major confluences exhibit any notable knickpoints, but the correlations between knickpoints, mapped landslides, and historic rockslide avalanche dams accounted for approximately 75% of the observed knickpoints, a surprising finding. These observations suggest that more detailed studies aided by high resolution data should be undertaken to further explore the characteristics of knickpoints triggered by tectonic uplift, local fault offset, bedrock erodibility, and landslide/rockslide dams.

Keywords Indus River · Landslide dam · Lithology · Knickpoint · DEM · Longitudinal profile

1 Introduction

Fluvial bedrock incision can exert significant impact on triggering catastrophic rockslides or sturzstroms that tend to choke river channels in steep mountainous terrain (Leopold et al. 1964; Whipple 2004). Previous studies on knickpoint migration through fluvial processes have suggested that their upstream migration assists in bedrock incision, and re-establishes local base level along the channels (Schumm 1977; Seidl and Dietrich 1994; Crosby et al. 2007; Ahmed and Rogers 2013; Rabin et al. 2015). In the absence of significant blockages ascribable to mass movement or active tectonic offset, most channels exhibit concave-upward longitudinal profiles, with channel gradients inversely proportional to tributary watershed area (Gannett 1901). Departures from this ideal profile can be exacerbated by active faulting, tectonic uplift, mass wasting processes, significant differences in lithology, or recent glaciation (Whipple and Tucker 1999; Keller 2002; Schoenbohm et al. 2004; Whipple 2004; Wobus et al. 2006; Korup et al. 2010).

Editorial handling: Ch. Schlüchter, G. Milnes and W. Winkler.

✉ Muhammad F. Ahmed
mfanr5@mst.edu

J. David Rogers
rogersda@mst.edu

Elamin H. Ismail
ehif22@mst.edu

[1] Department of Geological Engineering, University of Engineering and Technology, Lahore, Pakistan

[2] Department of Geosciences and Geological and Petroleum Engineering, Missouri University of Science and Technology, Rolla, MO, USA

Penck (1927) defined a knickpoint as a location along a river where a sharp change in channel profile is observed. The origin of knickpoints in a particular channel reach may be ascribable to multiple elements that combine to influence erosional equilibrium (Brush and Gordon 1960; Leopold et al. 1964). They have often been ascribed to geotectonic variables, such as fluvial processes, active faulting, folding or warping, abrupt lithologic contacts, localized ground settlement, and glacial activity (Korup 2004; Whipple 2004; Rabin et al. 2015). Figure 1 presents a schematic representation of the most common geomorphic triggers for knickpoints along stream channels, as viewed in longitudinal profile. Considerable effort is often required to differentiate knickpoints triggered by regional tectonic uplift, local fault offset, bedrock erodibility, and landslide/rockslide dams (Walsh et al. 2012).

1.1 Knickpoints along the river long profile

Figure 1a shows three common types of faults that can produce knickpoints, depending on the average rate of offset. Weaker knickpoints can also be associated with soft pockets of breccia and fault gouge along dormant or inactive faults. Profile (b) in Fig. 1 shows a typical fault graben, which can create 'bedrock shelves,' which can suddenly absorb runoff in thicker deposits of alluvium. Profile (c) illustrates the common impacts of persistent bedrock landslide and/or rock avalanche dams. Rapids formed by clusters of oversize 'skeletal blocks' are typical remnants of such channel blockages. Profile (d) shows typical impacts of man-made structures, such as dams, as well as earthquake-induced rockslide dams, like the Hunza blockage (2010).

1.2 Tectonic knickpoints

In tectonically active regions bedrock incision is the prime mechanism of locally increasing channel steepness, where there is an absence of detritus choking the channel (Sklar and Dietrich 2001; Kirby and Whipple 2001). The Himalayas are typified by high rates of tectonic uplift, which tend to increase steepness of the channel's longitudinal profile. Normal and thrust faulting often create steep knickpoints; especially when hanging walls drop in the downstream direction (e.g. reverse faulting with uplift on the downstream side), or when uplift occurs on the upstream block, relative to the downstream direction (see Fig. 1a).

Knickpoints are often observed where the active faults cross the river's longitudinal profile (Wobus et al. 2006). Numerous studies have observed a positive correlation between the rate of tectonic uplift and the normalized steepness index (Kirby and Ouimet 2011; Hodges et al. 2004; Wobus et al. 2006; Gani et al. 2007; Ismail and Abdelsalam 2012).

1.3 Lithologic knickpoints

Knickpoints may also develop in the absence of tectonics or geostatic/lithology change (Walsh et al. 2012; Ahmed and Rogers 2013). Seismically-induced rock slope failures sometimes occur irrespective of the formational contacts (Walsh et al. 2012). Lithologic units of varying resistance to the impacts of physical, chemical, and mechanical weathering can also account for the formation of knickpoints, although these are usually less prominent. Some of the physical factors promoting these features include the type and intensity of discontinuities perturbing the rock

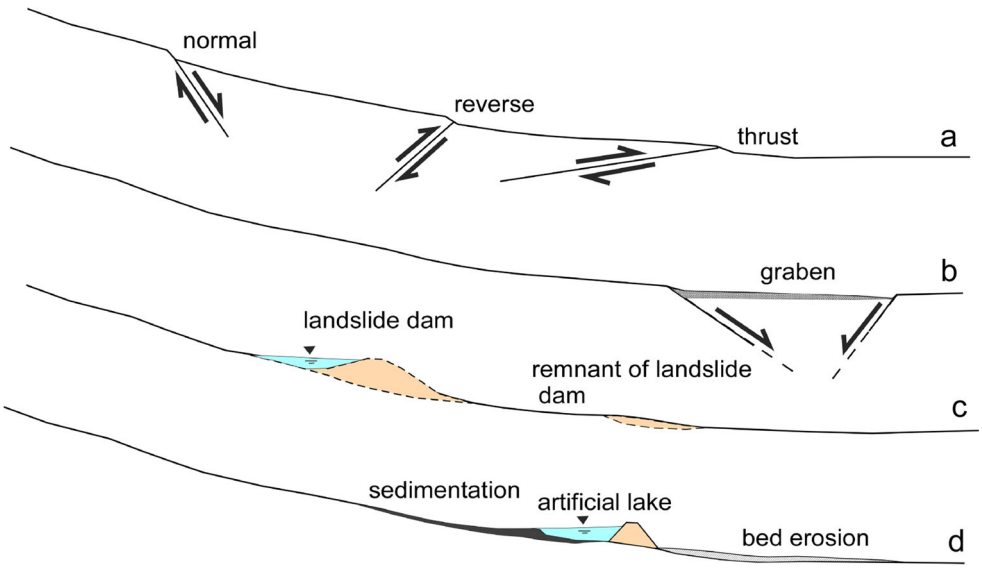

Fig. 1 Schematic representation of common geomorphic triggers for knickpoints along stream channels, as viewed in longitudinal profiles

mass (i.e. joint spacing, bedding plane or foliation orientation, faulting, bed thickness, and "sandwiching" of soft and hard units (Whipple et al. 2000; Borrelli et al. 2007). The more resistant lithologies tend to establish more robust and resilient knickpoints. Knickpoints also tend to occur at contacts between more and less competent rock types along the river profile (Walsh et al. 2012). Resistant strata underling steep channel reaches can occasionally generate remarkable knickpoints, such as Niagara or Victoria Falls. Channels can also become "hydraulically choked" by a continuous supply of coarse boulders, rock fragments, or cobbles, being discharged into the channel, often responsible for precipitous rapids, such as Hance and Crystal Rapids, as well as Lava Falls in the Grand Canyon of Arizona (Collins and Nash 1978).

1.4 Landslide knickpoints

The formation of temporary landslide dams and significant debris obstructions (see Fig. 1c, d), such as rockslides and rock avalanches, appear to be related to topography, lithology, structure, regional tectonics, and proximity to active or dormant faults (any pervasive horizons of low shear strength). Outbreak floods generally last only 12–24 h after initial overtopping, by quickly eroding landslide dams in the wake of initial overtopping (Lee and Duncan 1975). During the outbreak flood phase, large blocks of slide debris are broken up and tumbled downstream by the unusually high flows, but the peak outflow is usually very short lived, often leaving extremely large boulders and other 'coarse debris' that are not transported after the peak outflow subsides.

Bank undercutting during high flow events can undercut over-steepened slopes, often triggering mass wasting (Schumm 1977; Whipple et al. 2000). The size of these slope failures depends upon the local geology, topographic factors (e.g. slope morphology, tributary watershed area), tectonic activity, history of past landslippage, and climatic factors. If sufficient coarse debris fills the channel, a persistent flow obstruction can be formed at that location. This situation often occurs at the confluence of tributaries with main channels, or at the toe of large landslides (Crosby et al. 2007; Ahmed et al. 2015).

This regional exploratory study highlights the various geomorphic triggers that appear to play dominant roles influencing the formation of knickpoints along the upper Indus River. More detailed studies aided by high resolution data will be required to differentiate knickpoints triggered by regional tectonic uplift, local fault offset (e.g. gravity, step-over, and strike-slip faults), fluvial, and landslide dams.

2 Overview of the study area

The Upper Indus River watershed in northern Pakistan was selected for this regional level exploratory reconnaissance because the region is slated to be exploited for flood control and hydroelectric power generation facilities. The river's watershed area is 970,000 km^2, including 264,000 km^2 of mountainous catchment extending into the Tibetan Plateau. About 75,000 km^2 of its watershed lies within the boundaries of northern Pakistan, upstream of Tarbela Reservoir (see Fig. 2). The most notable tributaries in this region include the Shyok, Gilgit, Hunza, and Shigor Rivers. The region is perturbed by active thrust faults, low temperature–high pressure metamorphism, granitic batholiths, enigmatic syntaxes, deep gorges, and mélange belts of the Indus and Shyok sutures (Kazmi and Jan 1997; Ahmad et al. 2003).

Northern Pakistan lies upon a highly active subduction zone that has produced significant thrust faulting responsible for mountain building. The most notable faults include: the Main Karakoram Thrust (MKT) (the Shyok Suture Zone); Main Mantle Thrust (MMT), also known as the Indus Suture Zone; and the Main Boundary Thrust (MBT). These fault zones are the part of the Himalayan zone of convergence that resulted from the late Eocene to Early Oligocene collision of the active Eurasian and Indian plates. The presence of these thrust belts in the northwestern Himalaya are responsible for the high seismicity of the region (Kazmi and Jan 1997).

The Nanga Parbat-Haramosh Massif (NPHM) is a unique structural and topographic feature located in the northwestern corner of the Himalayas. The notable faults encountered along the Indus River in the NHPM region include the MMT, Raikot, Baroluma, and Stak Fault zones (Madin 1986). There are a few subsidiary faults and lineaments supposedly linked with these recognized fault zones. The MMT is an extensive fault zone composed of highly disintegrated remnants of metamorphic rocks, including various types of gneiss which are typical of subduction zones (Tahirkheli et al. 1979). The Raikot Fault is an active dextral reverse fault which extends northward from the Hunza Valley and passes west of Naga Parbat, to the unmapped portion of Kashmir to the south. The minimum horizontal slip of the Raikot fault is nearly 15 km, inferred from the Quaternary offset of the Indus River, with an uplift rate of $\sim$ 4 mm/year in the Holocene epoch (Madin 1986).

The NPHM region is subject to high rates of tectonic uplift (between 4 and 10 mm/year), as well as the highest documented rates of denudation and channel incision (less than or equal to 12 mm/year) in the world (Leland et al. 1998; Shehzad et al. 2009; Korup et al. 2010). The Indus

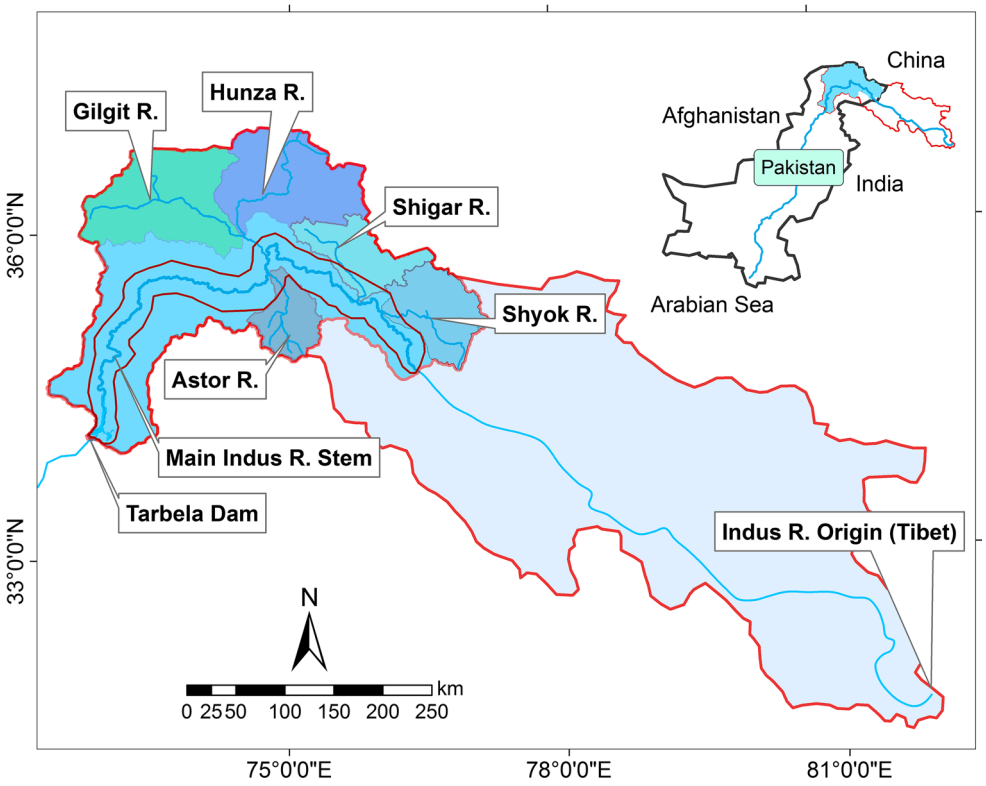

Fig. 2 The Upper Indus River Basin above Tarbela Dam and Reservoir is shown in blue (and outlined in red). The study area along the main stem of upper Indus River is outlined in brown

gorge is the deepest on Earth, reaching its maximum depths in the Patan and Dasu areas (Kazmi and Jan 1997). These exceptionally high rates of denudation and uplift may have removed half of the elevated crustal mass, exposing granitic plutons only a few million years old (Kazmi and Jan 1997).

The Geologic Map of Indus River Basin (Fig. 3) shows the mapped formations, which vary in age from Precambrian to Quaternary. These units include granites, granodiorites, quartz diorite, and hornblende gabbros of Miocene to Cretaceous-age in the Kohistan–Ladakh Batholith and associated plutons (reported as Tkb and Tkm on Fig. 3). The intrusion of NPHM region into the Eurasian plate (in the middle of the study area) has separated the Kohistan–Ladakh Batholith and plutons from the crystalline shield rocks of the Indian Plate (Tahirkheli et al. 1979; Dipietro et al. 2000). The NPHM region also includes rock units of Precambrian age in the Indian Basement Complex and Hazara–Kashmir Basement Complex (pCb). These units are chiefly comprised of highly weathered gneisses of various groups, graphitic blue and green schist facies, and amphibolites, etc.

The Jurassic–Cretaceous age Chilas Complex (KJc), Jurassic age Kamilla Amphibolites (Jk), and Precambrian sequence of metamorphic and sedimentary units of the Tanawal (pCt), Salkhala Formations (pEs) are exposed in the middle and lower reaches of the upper Indus River Basin.

The geologic units exhibiting significant mass wasting include the Precambrian Basement rocks (pCb) and Metasedimentary rocks (MPzm) in the Nanga Parbat Haramosh Massif, and the areas underlain by undifferentiated Precambrian age metamorphic rocks (pCs) and mixed Precambrian metamorphic and sedimentary rocks (pCt), in the lower reaches (Ahmed and Rogers 2014).

3 Data and methods

3.1 Stream power models for geomorphic analysis

In order to understand the morphology of the river's longitudinal profile, a variety of stream power models can be utilized (Montgomery 1994; Whipple 2004; Wobus et al. 2006). The basic stream power model for steady state conditions with respect to climate and uplift has been defined by the power law equation:

$$S = k_s A^{-\theta}, \quad (1)$$

where S is the local channel slope (gradient) of the river, A is the upstream drainage area, k_s is the local steepness index, which is the ratio of the channel gradient at specific locations (knickpoints) in the drainage area, and θ is the concavity of the stream channel profile (Kirby and Whipple 2001; Wobus et al. 2006; Kirby et al. 2007; Ismail and

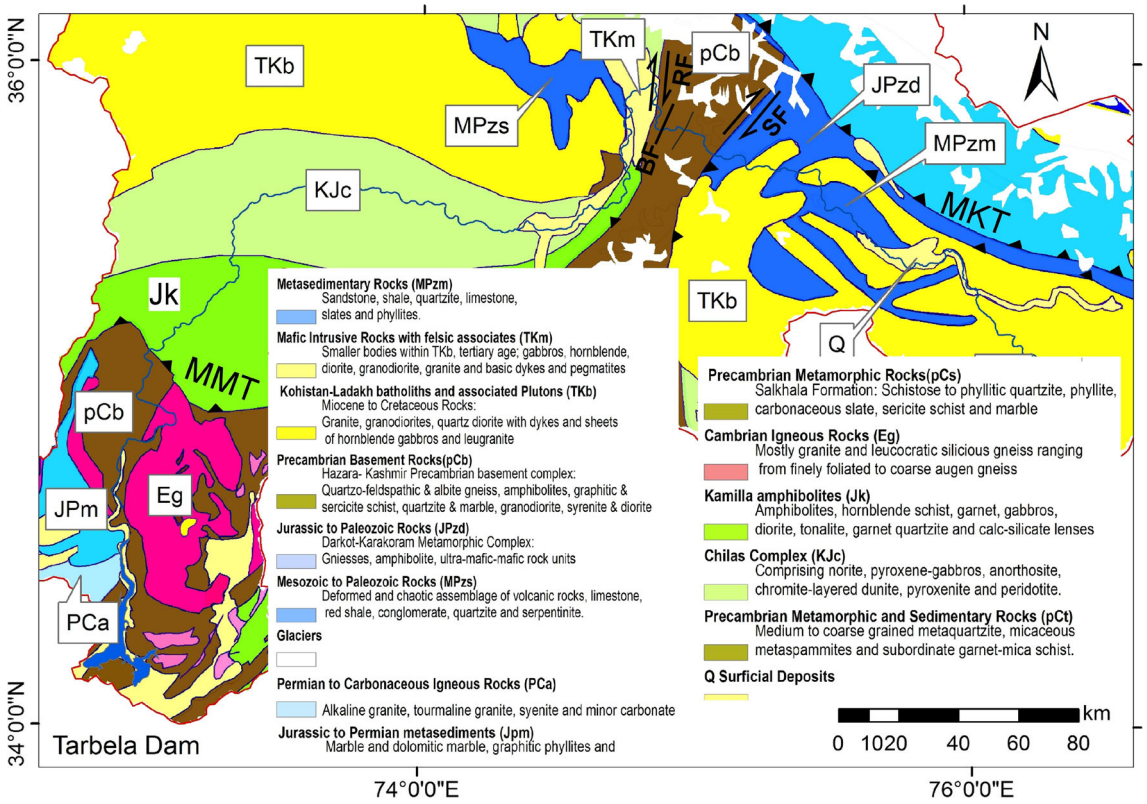

Fig. 3 Regional Geologic Map of the Upper Indus River Basin, within northern Pakistan (GSP 1993)

Abdelsalam 2012; Rabin et al. 2015). Furthermore, the normalized k_{sn}, which is the channel's steepness normalized to the upstream drainage area, can be calculated from the relationship given in Eq. 2 (from Whipple 2004)

$$k_{sn} = k_s A^{(\theta ref - \theta)}, \quad (2)$$

where θ_{ref} is the reference concavity and θ is the observed concavity of the stream channel. The θ_{ref} is channel concavity without considering any knickpoints along the channel profile, and can be computed by averaging the regional observed θ values of the respective channels in different reaches. The higher normalized k_{sn} values are generally attributed to areas of significant tectonic uplift, while lower values are more representative of fluvial river processes under conditions independent of tectonic activity (Whipple 2004). Korup (2004) adopted this approach to ascertain if the k_{sn} values of channel segments were influenced by rock avalanches, by noting if these values were significantly disparate within the remaining channel profile. The results obtained by Korup exhibited high k_{sn} values (up to $> 10^3$ $m^{0.9}$) for those channel reaches previously impacted by sizable rock slides.

3.2 Digital elevation model and landslide inventory mapping data

A regional level landslide inventory map was used as a database to compare the spatial distribution of knickpoints with mapped landslides of more than 0.5 km length (Ahmed and Rogers 2013, 2014). For the inventory mapping, a hill-shade topographic map was generated by utilizing ASTER GDEM Version 2 (Tachikawa et al. 2011) with 30 m resolution data (http://www.jspacesystems.or.jp/ersdac/GDEM/E/4.html) and topographic sheets with 40 m contour intervals. Anomalous topographic features normally associated with mass wasting processes were then identified, including: crenulated contours, divergent contours, topographic benches, and isolated knobs, etc. (Rogers 1994; Cruden and Varnes 1996; Glade 2001; Wills and McCrink 2002; Doyle and Rogers 2005; Ahmed and Rogers 2014).

3.3 Extraction of longitudinal profile and identification of knickpoints

The basic geomorphic analysis of the Indus River channel was performed using ArcGIS and Matlab software on georeferenced DEM data extracted from the ASTER GDEM v2 data, with 30 m resolution across the study area.

The drainage network and flow accumulation of the Indus River Basin were extracted using the Hydrology Module in ArcGIS software, and later these data files were imported into Matlab for further analysis.

Longitudinal profiles of the Indus River were extracted using the coded Stream Profiler 5.1 toolbar within ArcGIS 10.2 and Matlab 12a algorithm, downloaded from http://www.geomorphtools.org/Tools/StPro/Tutorials/StPro_UserGuidees_Final.pdf, and the equivalent longitudinal profile was extracted using River Tools using 30 m resolution ASTER GDEM v2 data. The extracted geomorphic information was obtained by employing stream power law equations (Hodges et al. 2004; Whipple 2004). In this study, a θ_{ref} value of 0.45 was adopted (following the recommendation of Whipple 2004), for the drainage systems of the Himalaya. The term $(\theta_{ref} - \theta)$ was calculated from the channel profile, considering the channel concavity at each point, and then used to estimate the normalized steepness index (k_{sn}) values. The user-identified knickpoints were marked on the extracted longitudinal profiles in Matlab software and their adjacent k_{sn} values were reported. As expected, a number of knickpoints with sharp vertical drops over short channel reaches were identified where mapped active faults cross the river channel.

4 Results and discussions

The user-identified knickpoints with their attributes were then exported to ArcGIS software to spatially compare their locations with mapped landslides and other geomorphic features along the Indus River to ascertain their possible association with them.

Figure 4 shows the overall distribution of knickpoints along the river with respect to change in elevation. A total of 251 knickpoints were identified at various locations along the upper Indus River (shown as the Main Indus R. stem in Fig. 2).

Figure 5 shows the relationship between tributary watershed area and flow distance from the upstream end of Tarbela Reservoir. The user identified knickpoints are shown as blue crosses in Fig. 5a, b. Actual elevations are shown in green, while smoothed elevations using 250 m averaged windows are shown in pink. The light blue line shows the predicted profile using the reference concavity value ($\theta_{ref} = 0.45$). The Indus River longitudinal profile is highly irregular and jagged because of active tectonics and mass wasting.

A similar version of the irregular Indus River longitudinal profile is presented in Fig. 6. Here the locations of major tributaries are shown by blue arrows, whose sizes are proportional to their respective watershed areas (At), and a few of the prehistoric landslide dams are delineated by red stars. The positions of active faults crossing the main channel are also marked on the profile, along with their approximate dips. Note the enlarged view of the longitudinal profile, showing two faults with major knickpoints, exhibiting k_{sn} values of 3225 and 2139 respectively, a few kilometers upstream of the NPHM region. These knickpoints may have developed from subsidiary faulting linked with the MMT zone in the NPHM region.

In Fig. 7 major profile anomalies can be discerned by knickpoint clustering in the NHPM region, which is undergoing high rates of tectonic uplift because of its proximity to the active subduction zone. The topographic relief along the main channel in this area reaches depths in excess of 6500 m. This spatial distribution of k_{sn} values suggests that the increased tectonic activity in the NHPM region has triggered significant knickpoints along the Raikot, Baroluma, and Stak thrust faults. In the Raikot fault zone the knickpoints achieved the highest k_{sn} values of 2248–4169. In vicinity of the Baroluma and Stak Faults the k_{sn} intensities were up to 4196. Knickpoints with low to

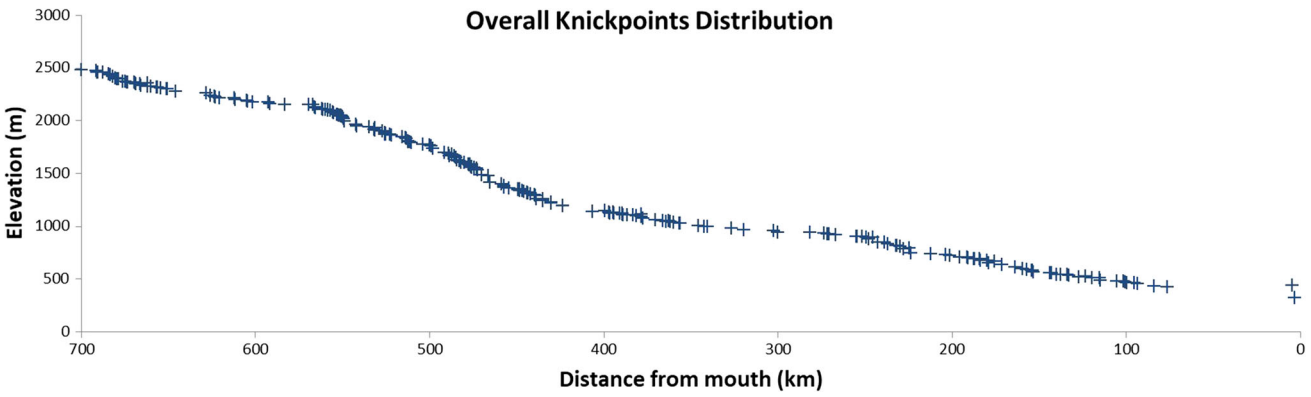

Fig. 4 Knickpoint distribution with elevation along the longitudinal profile of the upper Indus River upstream of Tarbela Dam reservoir

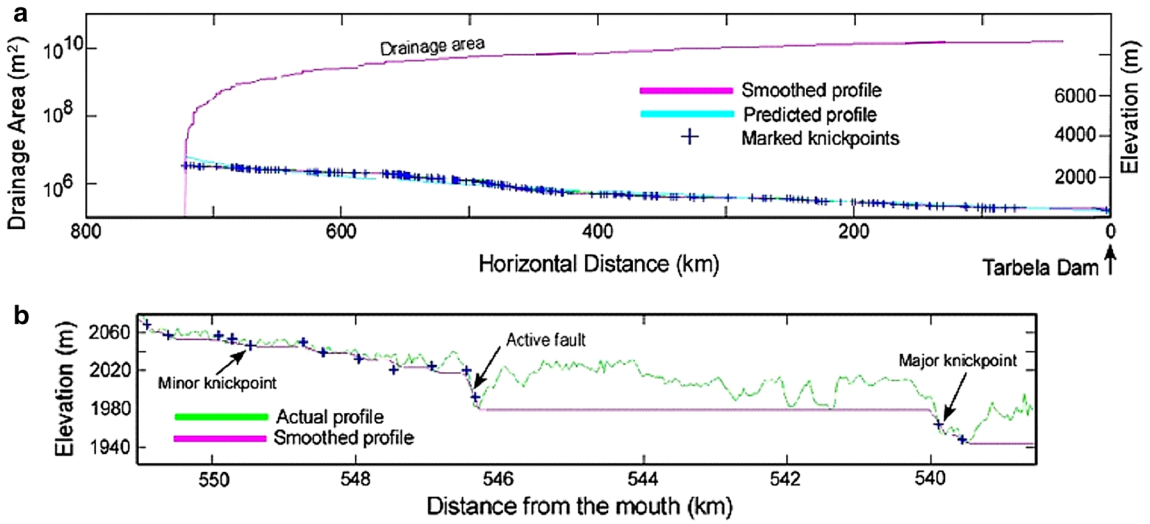

Fig. 5 **a** Longitudinal profile of the Indus River upstream of Tarbela Dam generated by Matlab 2012a, using ASTER DEM 30 m resolution data: **b** shows an enlarged portion of the plot, illustrating the observed and predicted channel profiles with user-specified knickpoints

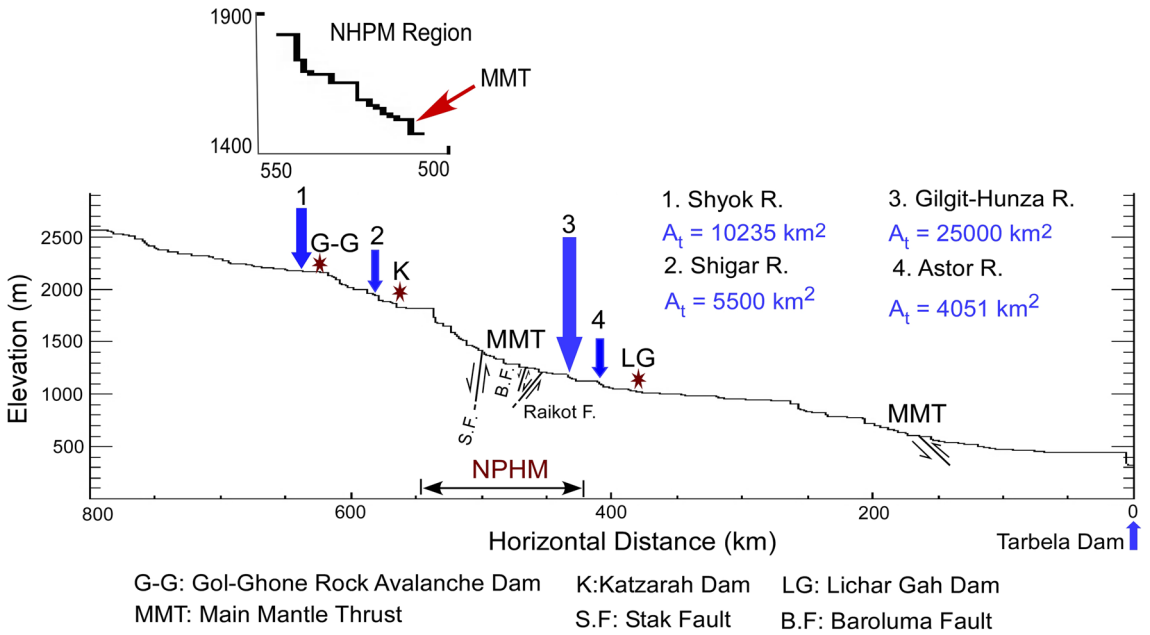

Fig. 6 Longitudinal profile of upper Indus River extracted from ASTER DEM 30 m resolution data using River Tools software

moderate signals are rarely associated with thrust faults (Rabin et al. 2015).

Figure 8 presents the variation of normalized k_{sn} values, extracted from the 251 knickpoints identified along the channel. This plot presents automated calculations of channel normalized steepness index (shown as hollow circles) adjacent to the significant knickpoints. The various geologic formations are shown in different colors and active faults are denoted as dotted lines, where the Indus River crosses these features. The vertical lines on the diagram shown in blue denote the locations of major tributary entries discharging into the Indus River, while thin lines (marked with light blue) denote prominent landslide dam features with their respective k_{sn} values. The boundaries between different geologic formations and major thrust faults were extracted from the Geologic Map of Northern Pakistan at a scale 1:1,000,000 (Geological Survey of Pakistan 1993). This information, along with the tributary river junction locations, was then overlapped on the Indus River's longitudinal profile to evaluate the spatial distribution of knickpoints and variations in normalized steepness index (k_{sn}) with various geomorphic triggers.

The geomorphic reconnaissance revealed an interesting comparison between knickpoints and various geomorphic

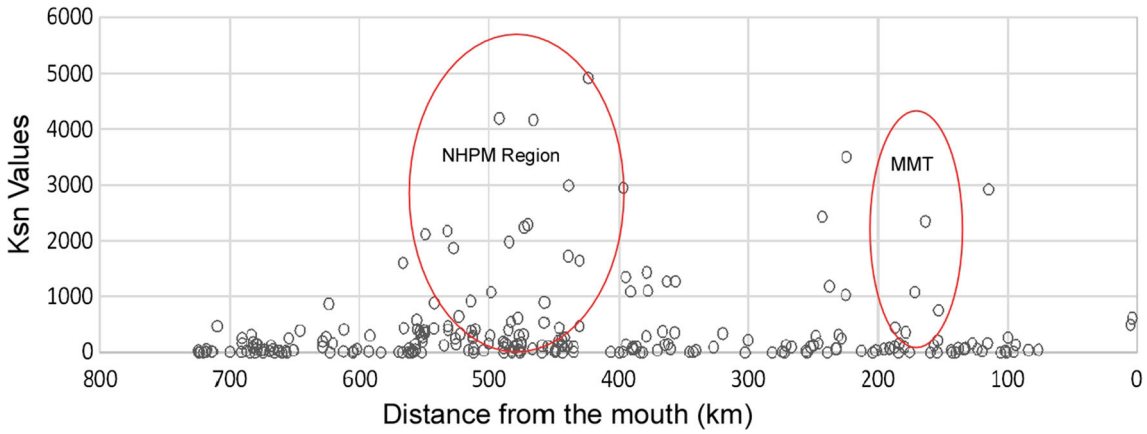

Fig. 7 Distribution of k_{sn} values with respect to their relative distance from the mouth along the Indus River channel profile

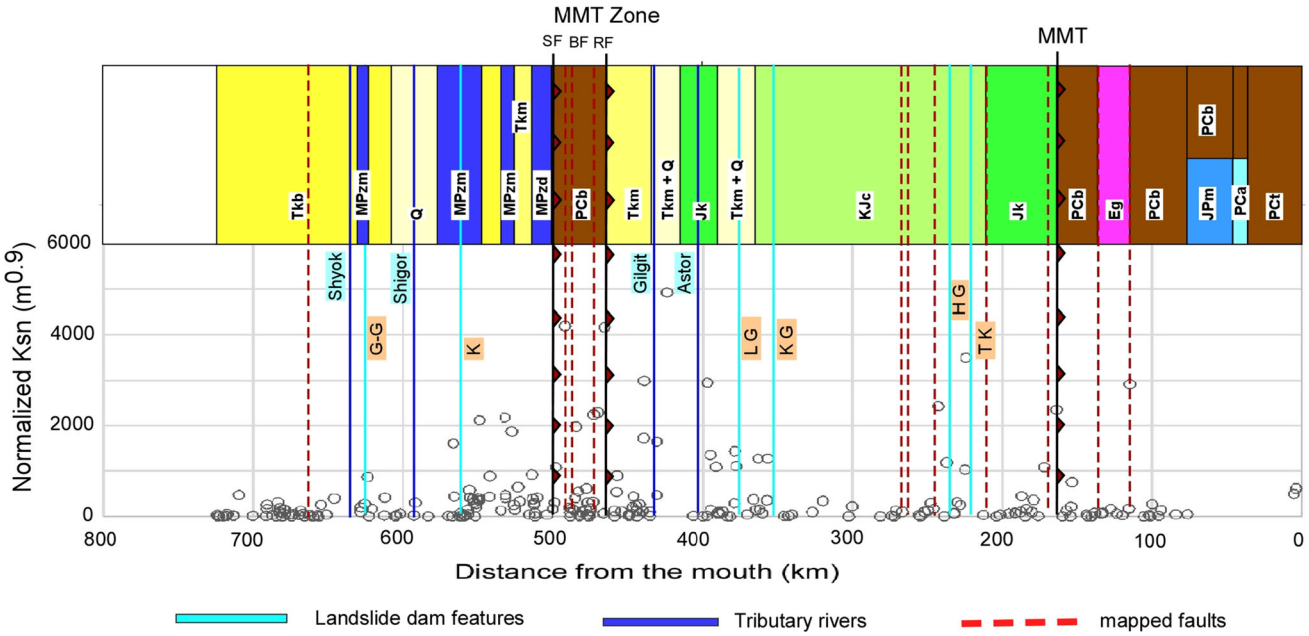

Fig. 8 Plot illustrating the comparison of exposed geologic formations (see Fig. 3) and other geomorphic parameters along the longitudinal profile of the Indus River upstream of Tarbela Dam, extracted from ASTER DEM 30 m data using Matlab 12a. Note that MMT fault zone, Stak SF, Baroluma BF, Raikot RF, and other faults exhibit high k_{sn} values where the river crosses these faults

features on a regional scale. The knickpoints with noticeable k_{sn} values at particular locations (along the longitudinal profile of the Indus River) suggests landslide dams as the most frequent causal factor, not tectonic uplift.

The regional scale landslide inventory map identified 451 landslide and rockslide avalanche features more than half kilometer in length have likely impacted the Indus River channel (Ahmed and Rogers 2012, 2014). The slope morphologies at the landslide dam sites are indicative of large scale perturbation of the hill slopes by past episodic activities of mass wasting, which often form ephemeral landslide dams. These features tend to be structurally-controlled as a result of intense foliation, discontinuity suites, lithologic contacts, and active faults. Figure 9 shows the location of the observed knickpoints with the landslide inventory map (Ahmed and Rogers 2014). The size of knickpoints are shown as graduated symbols with respect to their normalized steepness index (k_{sn}) values. A few reaches along the Indus River exhibit anomalously high k_{sn} values. These are highlighted where the active thrust faults (particularly in the NPHM region), rockslide avalanches, and translational bedrock landslides revealed their likely association with observed knickpoints.

Figure 10a shows an excerpt of the landslide inventory map, within the NPHM region. The pattern of knickpoints (as shown in Fig. 5) exhibits the highest clustering ($\sim$ 52%) where the Indus River flows nearly 130 km through the seismically active NPHM region. Knickpoints

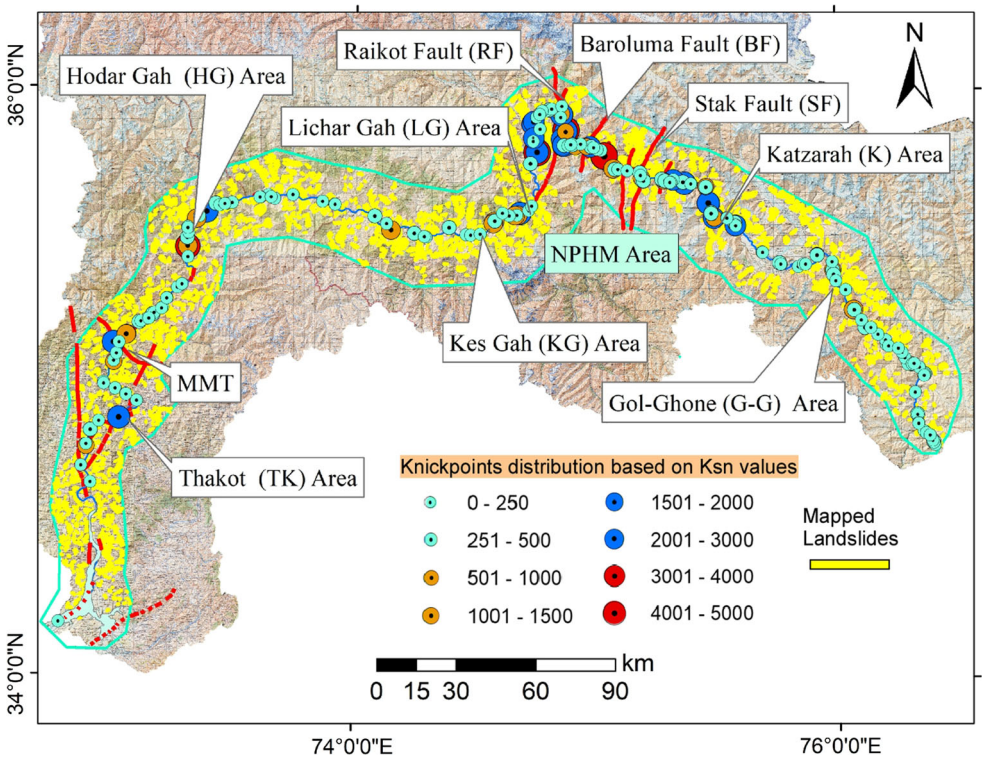

Fig. 9 Landslide inventory map with graduated symbols denoting the size of the exported knickpoints in terms of their relative k_{sn} values. The highlighted areas reveal a likely association between observed knickpoints and historic landslide dam sites

in this reach are likely ascribable to a combination of increased tectonic uplift, active faulting, and a higher concentration of mass wasting. The highest values of k_{sn} were noticed where the Indus River profile crosses the MMT and other significant faults, or where it intersects fault lineaments. Figure 10b shows the location of the Indus River where it flows along the Raikot Fault in the NPHM region. Numerous offsets are distributed within the 1–2 km of the main fault trace (Madin 1986), which is indicative of high erosion rates that have resulted in straightening the Indus River channel in that vicinity. The Indus River then flows north along the Raikot fault to the Sassi area, where it turns about 140° to the west, towards the area south of the NPHM region. Zeitler et al. (1982) concluded that a rapid uplift of this area commenced in late Miocene time. One of the highest k_{sn} value knickpoints was observed along the channel in this narrow, steep-sided gorge, which is one of the best examples of bedrock incision along the upper Indus River.

A few examples of mega landslide dams (volumes greater than 10 million m^3) have been reported along the Indus River (Shroder and Bishop 1998; Hewitt 2002; Hewitt et al. 2011), Fig. 11 shows the location of prehistoric Katzarah rock avalanche dam (Hewitt et al. 2011), where some major knickpoints were observed in the breached section. In this area the river is currently flowing well above its pre-landslide dam level (Hewitt et al. 2011).

Figure 12 shows the upstream location of Lichar Gah area where a significant landslide was triggered by an earthquake in 1841, forming a natural dam along the Indus River (Code and Sirhindi 1986). The dam was initially breached 6 months later, flooding the channel for hundreds of kilometers downstream. A few kilometers upstream of the old landslide dam lies a rapidly dissected section of the sediments deposited in the short-lived reservoir. Significant knickpoints were observed along the channel profile, which are sourced from the breach of this temporary barrier.

The cumulative frequency distribution of all of the knickpoints are presented in Fig. 13. The plot shows that the maximum k_{sn} value reaches 4916, but 84% of the k_{sn} values are less than 500. The graph also shows that 10% of the k_{sn} values are greater than 1000, which is a significant figure in comparison to knickpoints world-wide. 50% of the k_{sn} values are less than 1000, many which occur downstream of the tectonically active NHPM region. Knickpoints with moderate k_{sn} values are distributed across the entire watershed, especially in the upper reaches. Some of these may be partially influenced by rapid glacial melting and retreat, as well as ice dam failures. The knickpoints with higher k_{sn} values, including a few with highest k_{sn} values > 4000, are located along the 100 km long reach passing through the NHPM region, where active faulting occurs. A larger number of landslide related features were identified in this same reach, which further highlights the significance of both triggers (tectonic offset and mass wasting).

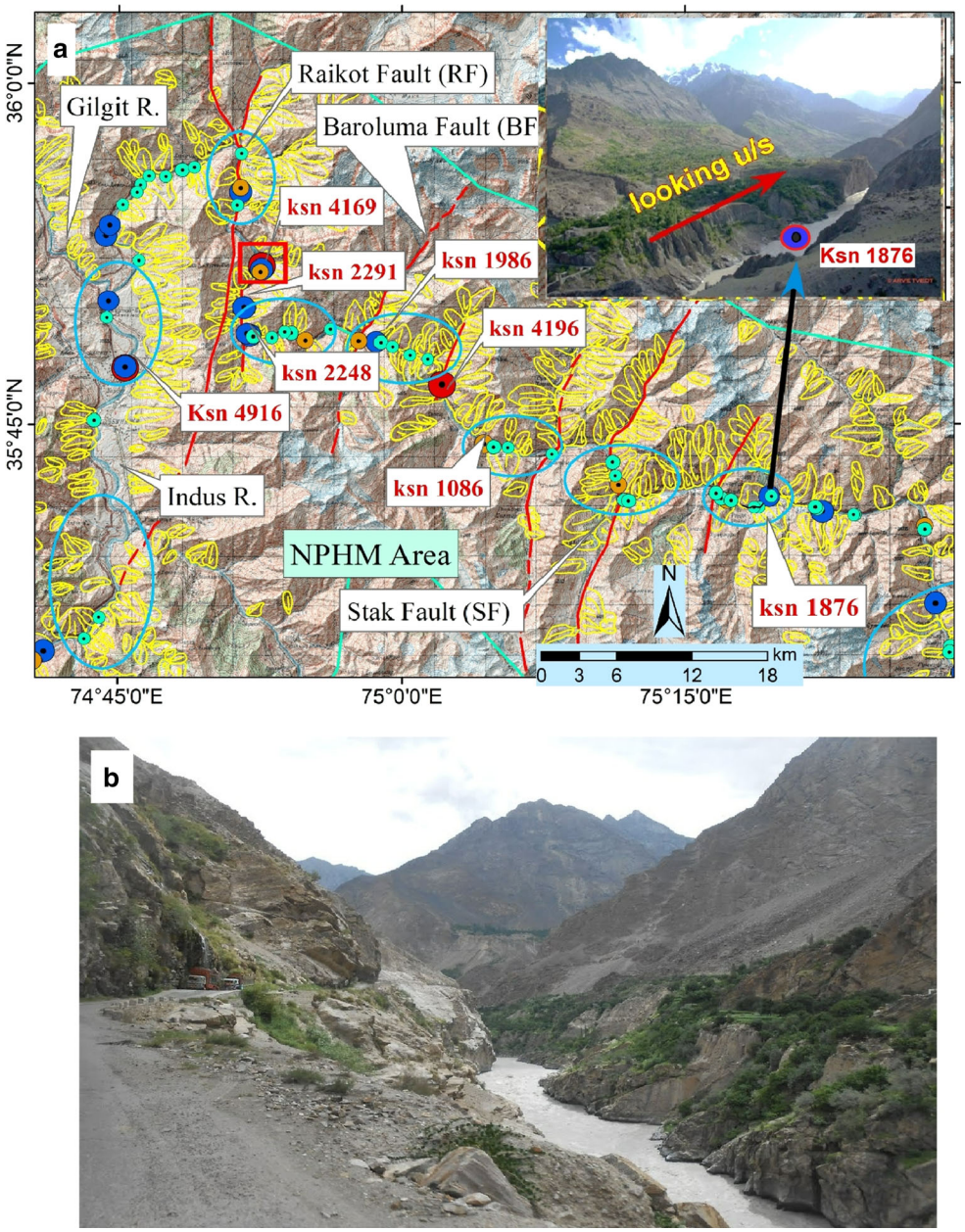

Fig. 10 **a** Section of the landslide inventory map showing the mapped landslides, active faults, and identified knickpoints with graduated circles indicative of the size of the observed k_{sn} values. The imbedded image is a photo of the breached section of a landslide dam with the location of an knickpoint exhibiting a significant k_{sn} value: **b** shows the example of deep bedrock incision where the Indus River flows along the Raikot Fault Zone in NPHM region [the location of the photo is shown as red square box in the Fig. 10a (photo credit Nigyal AB, 2014)]

The careful observations made in this study suggests that the larger prehistoric rockslide avalanches, like those at Katzarah (KT Z), Gol–Ghone (G–G), Lichar Gah (L G), Kes Gah (K G), and Hodar Gah (H G), the normalized steepness index (k_{sn}) increases markedly (see Fig. 8).

After evaluating the likely trigger factors contributing to the formation of knickpoints, all of the user identified knickpoints were sorted by groups. Figure 14 shows the overall distribution of the knickpoints based on spatial correlations between various trigger factors. The analysis shows that landslides and active faults are the major contributing factors responsible for knickpoints, which also engenders highly irregular and obstructed channel profile. A few knickpoints were identified across the alternating bands of less resistant (i.e. MPzm, MPzs and pCb) and more resistant geologic formations (i.e. Tkm and Tkb), between the MMT (Raikot fault zone) and the Stak shear fault zone, in the NPHM region. But, the lithologic contacts exhibited poor correlations with identified knickpoints, except where active thrust faults form the mapped unit boundaries (see Fig. 8). The abundance of rock debris and clastic sediments are likely the result of frequent landslide damming along the channel, which may have overprinted the expected effects of lithologic contrasts at various locations.

The tributary river junctions denoted on Fig. 8 did not exhibit any noticeable correlation with the observed knickpoints. Downstream of the Gilgit–Indus River

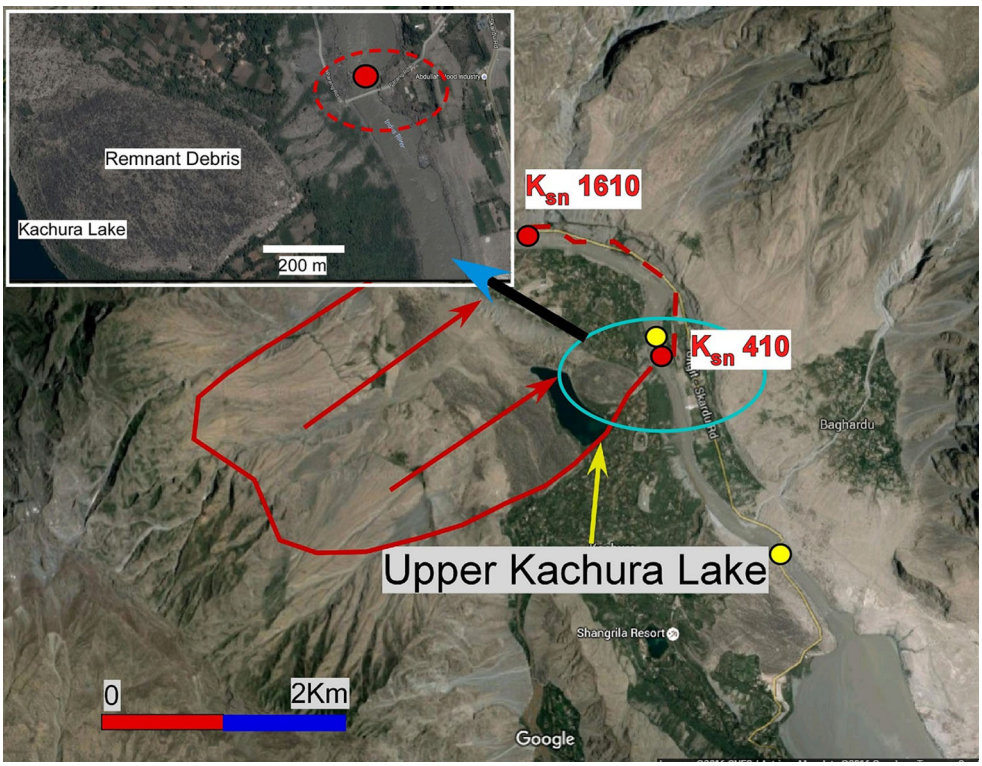

Fig. 11 Google map view of the historic Katzarah Rock avalanche dam site. The sudden change in the width of the river is a telltale sign of past debris blockages. The zoomed image in the left corner shows a remnant lake, Upper Kachura, that was preserved during the catastrophic breaching of this rock avalanche dam. A few major knickpoints were identified here, testifying to this recent historic event

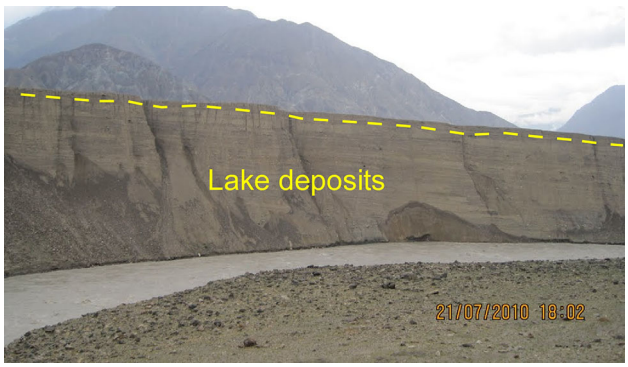

Fig. 12 Thick accumulation of the lake deposits a few kilometer upstream of the Lichar Gah Landslide dam. The Indus River might have incised itself during the likely breach of this natural dam (photo credit Mughal A 2010)

confluence a significant knickpoint was noted with an extremely high k_{sn} value (4900 $m^{0.9}$). This feature may have developed from subsidiary faulting linked with Raikot fault, or could be influenced by the triple junction of Himalayan, Karakoram, and Hindukush Ranges.

Figure 15 summarizes the tentative distribution of knickpoints with respect to the various geomorphic features likely responsible for creating them. About 62% of the observed knickpoints exhibit spatial agreement with mapped and/or documented landslides, while 27% seemed to correlate with landslides and/or faults crossing the Indus River. There was no significant correlation identified between the observed knickpoints and lithologic unit contacts exposed along the river (~ 3%). Lithologic units of varying resistance to erosion can also account for the formation of knickpoints, although these appear to be less prominent. For this study, the only geologic variable was mapped bedrock lithology and age (at a scale of 1:1,000,000), and not secondary structures, such as joint suites, folding, warping, inactive faults, breccia, and cataclastic shear zones, or rapid glacial unloading. A meaningful correlation could only be established by including spatial information diagnostic of each rock unit encountered along the river channel. This may explain the poor correlation between observed knickpoints and geologic formations in the study. 8% of the observed knickpoints did not exhibit any noticeable correlations with the recognized geomorphic factors at the regional scale of the study area (described previously).

These comparisons highlight the significance of the various geomorphic features contributing to knickpoint initiation along the Indus River in the Himalayas of northern Pakistan. The paucity of reliable topographic and geologic data and relative inaccessibility of the study area necessitated the use of large scale maps and interpretations, which are now beginning to undergo more detailed evaluations, on-the-ground. The authors believe that the desktop study described herein was a suitable place to initiate a reconnaissance level examination of mass wasting processes, where the features were "blindly mapped," and

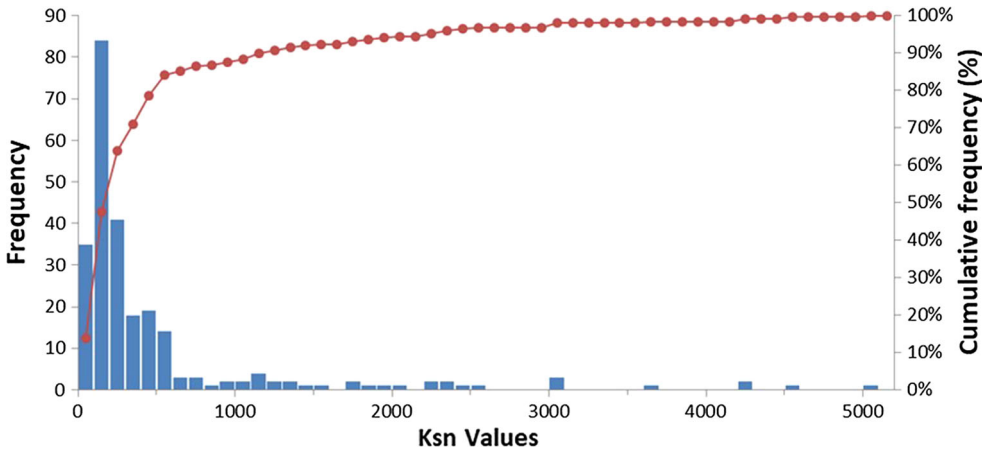

Fig. 13 This diagram shows the overall frequency distribution of the knickpoints with respect to normalized steepness index (k_{sn}) values

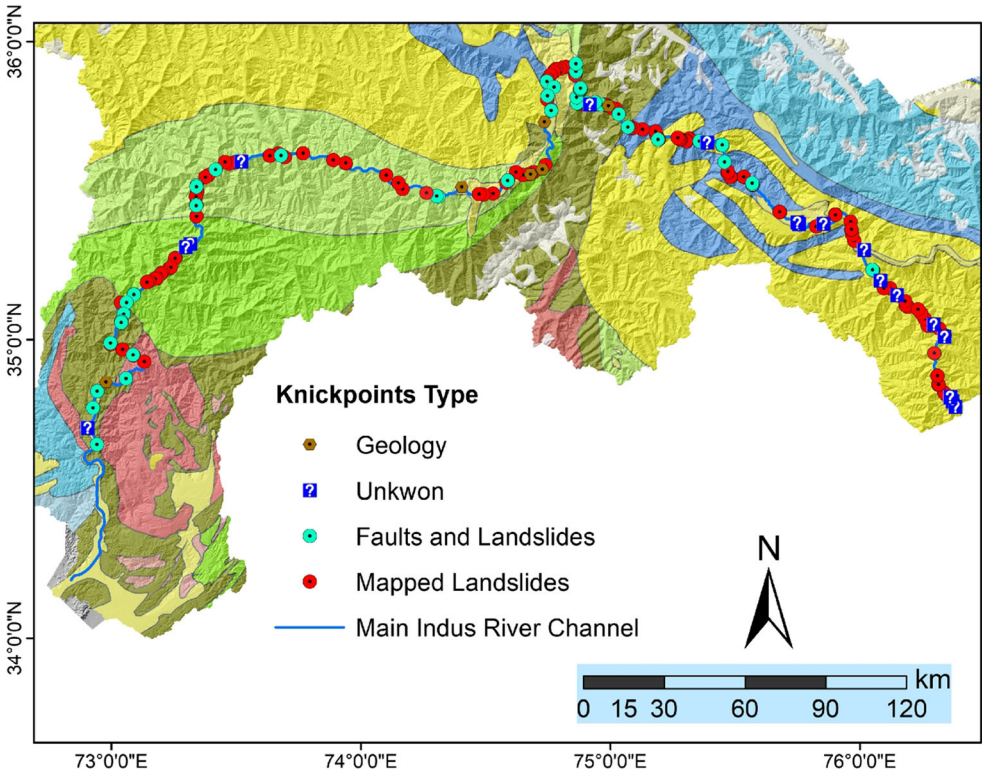

Fig. 14 The distribution of the knickpoints on the hillshade geologic map, based on the various geomorphic factors. After a careful screening analysis of identified knickpoints, these could be categorized into different groups, described in the legend

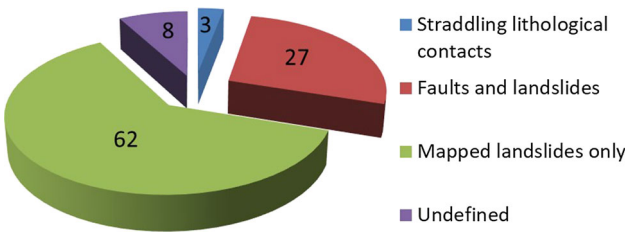

Fig. 15 Pie chart illustrating the distribution of knickpoints with respect to various geomorphic features

then compared to historic and prehistoric landslide features. More detailed site-specific analyses would need to be undertaken with medium to high resolution data (DEM with 10 m resolution) to verify the assumptions gleaned in large measure from identification of anomalous topography (identifying landslide features) and perturbations of the channel profile (identifying knickpoints).

5 Conclusions

This study was conducted to explore the use of low cost regional remote sensing data for the investigation of the likely roles of different geomorphic variables influencing the formation of significant knickpoints observed along the upper Indus River.

The knickpoints and their related geomorphic parameters (channel profile, concavity, drainage area and steepness index, etc.) were extracted from the analysis of ASTER Digital Elevation Models (DEMs) with 30 m resolution using ArcGIS, River Tools and Matlab software. 251 major and minor knickpoints were extracted along the river's longitudinal profile, extending ~ 750 km long upstream of Tarbela Reservoir. The knickpoint locations and their respective normalized steepness index (k_{sn} values) were compared with the bedrock lithology, mapped faults, regional level landslide inventory maps, and the locations of historic rockslides.

The analysis suggests that; (1) the highest clustering of knickpoints (~ 52%) occurs along the 130 km long reach where the Indus River crosses the NPHM. Exceptionally high values of k_{sn} (between 2000–4900 $m^{0.9}$) were observed where the mapped landslides coincide with active faults (i.e. MMT, Raikot, Baroluma, and Stak faults) crossing the channel. (2) The locations of identified knickpoints were also compared with the entry points of major tributaries of the Indus River, where large influxes of sediment would be expected to constrict the main channel. This evaluation does not show any meaningful correlation with the observed knickpoints. (3) The identified knickpoints exhibit a good correlation with geologic contacts controlled by recognized active faults. (4) The correlations between spatial locations of knickpoints, mapped, and documented rockslide dams revealed moderate to high normalized steepness index (k_{sn}) values on several landslide debris dam sites, particularly in the Gol–Ghone (k_{sn} 877), Katzarah (k_{sn} 1610), Lichar Gah (k_{sn} 2951), and Kes Gah (k_{sn} 1278) events.

The cumulative frequency distribution of all of the knickpoints shows that the maximum k_{sn} value was 4916, but 84% of the k_{sn} values were found to be less than 500. 10% of the measured k_{sn} values were greater than 1000, which is a significant figure. The knickpoints with higher k_{sn} values, including a few with k_{sn} values greater than 4000, are located in the NHPM region where active thrust faults are recognized. A larger number of landslide related features were also identified in this region, which further highlights the significance of both of these controlling factors.

The overall sorting and spatial distribution of knickpoints with respect to evaluated geomorphic features reveals that about 62% of the knickpoints exhibit spatial agreement with mapped and/or documented rock slides; and 27% correlate with mapped landslides where active faults cross or run along the Indus River. Only 8% of the identified knickpoints did not exhibit any spatial correlation with the above-cited factors. The results of this exploratory study concluded that landslide dams and active thrust faults appear to be the major trigger factors of the knickpoints along the Indus River's longitudinal profile.

Further studies aided with high resolution data would likely be more beneficial in differentiating knickpoints triggered by regional tectonic uplift, local fault offset, bedrock erodibility (fluvial processes), and/or landslide/rockslide dams.

Acknowledgements The authors are thankful to Natural Hazards Mitigation Institute at the Missouri University of Science and Technology in Rolla, MO, USA, for providing an opportunity to accomplish this work. The authors would also like to thank University of Engineering and Technology, Lahore, Pakistan for financial support to one of the authors to conduct this research.

References

Ahmad, I., Jan, M. Q., & Dipietro, A. (2003). Age and tectonic implications of granitoid from the Indian Plate of northern Pakistan. *Journal of the Virtual Explorer*, *11*, 21–28.

Ahmed, M. F., & Rogers, J. D. (2012). *Landslide mapping and identification of old landslide dams along the Indus River in Pakistan, using GIS techniques*. Association of Environmental and Engineering Geologists 55th annual meeting, Salt Lake City, Utah, Sept. 22–27 (Vol. 55, p. 44).

Ahmed, M. F., & Rogers, J. D. (2013). *Thalweg profiles and knickpoints as useful discriminators of prehistoric landslide dams in Northern Pakistan*. 125th Annual meeting Geological Society of America, Denver Colorado, Oct 24–28 (Vol. 45, No. 7).

Ahmed, M. F., & Rogers, J. D. (2014). Creating reliable, first-approximation landslide inventory maps using ASTER DEM data and geomorphic indicators, an example from the upper Indus River in northern Pakistan. *Journal of Environmental & Engineering Geoscience, 20,* 67–83.

Ahmed, M. F., Rogers, J. D., & Ismail, E. H. (2015). Historic landslide dams along the Upper Indus River, Northern Pakistan. *Natural Hazards Review*, *16*(3), 04014029. https://doi.org/10.1061/(ASCE)NH.1527-6996.0000165.

Borrelli, L., Greco, R., & Gulla, G. (2007). Weathering grade of rock masses as a predisposing factor to slope instabilities: Reconnaissance and control procedures. *Geomorphology, 87,* 158–175.

Brush, L. M., & Gordon, W. M. (1960). Knickpoint behavior in noncohesive material: A laboratory study. *Geological Society of America Bulletin, 71,* 59–73.

Code, J. A., & Sirhindi, S. (1986). Engineering implications of the impoundment of the Indus River by an earthquake induced landslide. In R. L. Schuster (Ed.), *Landslide dams, risk, and mitigation* (pp. 97–110). ASCE Geotechnical Special Publication (GSP) 3.

Collins, R. O., & Nash, R. (1978). *The big drops: Ten legendary rapids of the American West*. San Francisco: Sierra Club Books.

Crosby, B. T., Whipple, K., Gasparini, N. M., & Wobus, C. W. (2007). Formation of fluvial hanging valleys: Theory and simulation. *Journal of Geophysical Research, 112,* 1–20.

Cruden, D. M., & Varnes, D. J. (1996). Landslide types and processes. In A. K. Turner, & R. L. Schuster (Eds.), *Landslides, investigation and mitigation* (pp. 36–75). Special Report 247. Washington, DC: Transportation Research Board.

Dipietro, J. A., Hussain, A., Ahmad, I., & Khan, M. A. (2000). The main mantle thrust in Pakistan: its character and extent. In: M. A. Khan, P. J. Treloar, M. P. Searle, & M. Q. Jan (Eds.), *Tectonics of the Nanga Parbat syntaxis and the western Himalaya* (pp. 375–393). Geological Society of London Special Publication No. 170.

Doyle, B. C., & Rogers, J. D. (2005). Seismically-induced lateral spread features in the western New Madrid seismic zone. *Environmental & Engineering Geoscience*, *XI*(3), 251–258.

Gani, N. D., Gani, M. R., & Abdelsalam, M. G. (2007). Blue Nile incision on the Ethiopian plateau: Pulsed plateau growth, Pliocene uplift, and hominin evolution. *Geological Society America Today, 17,* 4–11.

Gannett, H. (1901). Profiles of rivers in the United States: United States Geological Survey Water Supply Paper No. 44.

Glade, T. (2001). Landslide hazard assessment and historical landslide data: an inseparable couple? In T. Glade, P. Albini, & F. Frances (Eds.), *The use of historical data in natural hazard assessments* (pp. 153–167). Berlin: Springer.

Hewitt, K. (2002). Styles of rock-avalanche depositional complexes conditioned by very rugged terrain, Karakoram Himalaya, Pakistan. In S. G. Evans & J. V. Degraff (Eds.), *Catastrophic landslides: Effects, occurrence, and mechanism* (Vol. XV, pp. 345–377)., Reviews in engineering geology Boulder: Geological Society of America.

Hewitt, K., Gosse, J., & Clague, J. J. (2011). Rock avalanches and the pace of late Quaternary development of river valleys in the Karakoram Himalaya. *Geological Society of America Bulletin, 123,* 1836–1850.

Hodges, K. V., Wobus, C., Ruhl, K., Schildgen, T., & Whipple, K. (2004). Quaternary deformation, river steepening, and heavy precipitation at the front of the Higher Himalayan ranges. *Earth Planet Science Letters, 220,* 379–389.

Ismail, E. H., & Abdelsalam, M. G. (2012). Morpho-tectonic analysis of the Tekeze River and the Blue Nile drainage systems on the Northwestern Plateau, Ethiopia. *Journal of African Earth Sciences, 69,* 34–47.

Kazmi, A. H., & Jan, M. Q. (1997). *Geology and tectonics of Pakistan*. Karachi: Graphic Publishers.

Keller, E. A. (2002). *Active tectonics: Earthquakes, uplift, and landscape*. Upper Saddle River: Prentice Hall.

Kirby, E. N., Harkins, E., Wang, X., Shi, C., & Fan Burbank, D. (2007). Slip rate gradients along the eastern Kunlun fault. *Tectonics, 26,* 1–16.

Kirby, E., & Ouimet, W. (2011). Tectonic geomorphology along the eastern margin of Tibet: Insights into the pattern and processes of active deformation adjacent to the Sichuan Basin. *Geological Society Special Publication, 353,* 165–188.

Kirby, E., & Whipple, K. X. (2001). Quantifying differential rock-uplift rates via stream profile analysis. *Geology, 29,* 415–418.

Korup, O. (2004). Landslide-induced river channel avulsions in mountain catchments of southwest New Zealand. *Geomorphology, 63,* 57–80.

Korup, O., Montgomery, D. R., & Hewitt, K. (2010). Glacier and landslide feedbacks to topographic relief in the Himalayan syntaxes. *Proceedings of National Academy of Sciences USA, 107,* 5317–5322.

Lee, K. L., & Duncan, J. M. (1975). *Landslide of April 25, 1974 on the Mantaro River*. Peru/Washington, DC: Report of Inspection/National Academy Press. https://doi.org/10.17226/20646.

Leland, J., Reid, M. R., Burbank, D. W., Finkel, R., & Caffee, M. (1998). Incision and differential bedrock uplift along the Indus River near Nanga Parbat, Pakistan Himalaya, from ^{10}Be and ^{26}Al exposure age dating of bedrock straths. *Earth and Planetary Science Letters, 154,* 93–107.

Leopold, L. B., Wolman, M. G., & Miller, J. P. (1964). *Fluvial processes in geomorphology*. San Francisco: W.H. Freeman.

Madin, I. P. (1986). Structure and neotectonics of the Northwestern Nanga Parbat-Haramosh Massif. MS thesis, Oregon University, USA.

Montgomery, D. R. (1994). Valley incision and the uplift of mountain peaks. *Journal of Geophysical Research, 99,* 13913–13921.

Penck, W. (1927). *Die morphologische Analyse ("Morphological analysis of landforms"): Stuttgart* (English translation in 1953 by H. Czech & K. C. Boswell). London: Macmillan.

Rabin, M., Sue, C., Valla, P. G., Champagnac, J. D., Carry, N., Bichet, V., et al. (2015). Deciphering neotectonics from river profile analysis in the karst Jura Mountains (northern Alpine foreland). *Swiss Journal of Geosciences, 108,* 401–424.

Rogers, J. D. (1994). *Report accompanying map of landslides and other surficial deposits of the city of Orinda* (p. 141). CA: Rogers/Pacific, Inc. for the City of Orinda Public Works Department.

Schoenbohm, L. M., Whipple, K. X., Burchfiel, B. C., & Chen, L. (2004). Geomorphic constraints on surface uplift, exhumation, and plateau growth in the Red River region, Yunnan Province, China. *Geological Society of America Bulletin, 116*(7), 895–909.

Schumm, S. A. (1977). *The Fluvial System*. New York: Wiley.

Seidl, M. A., & Dietrich, W. E. (1994). Longitudinal profile development into bedrock: An analysis of Hawaiian channels. *Journal of Geology, 102,* 457–474.

Shehzad, F., Mahmood, S. A., & Gloaguen, R. (2009). Drainage network and seismological analysis of active tectonics in the Nanga Parbat Haramosh Massif, Pakistan. In *IEEE geosciences and remote sensing symposium, July 12–17* (pp. 9–12).

Shroder, J. F., & Jr, Bishop. (1998). Mass movement in the Himalaya: New insights and research directions. *Geomorphology, 26,* 13–35.

Sklar, L., & Dietrich, W. E. (2001). Sediment and rock strength controls on river incision into bedrock. *Geology*, *29*(12), 1087–1090.

Tachikawa, T., Kaku, M., Iwasaki, A., Gesch, D., Oimoen, M., Zhang, Z., Danielson, J., Krieger, T., Curtis, B., Haase, J., Abrams, M., Crippen, R., & Carabajal, C. (2011). *ASTER global digital elevation model version 2—Summary of validation results* (pp. 15–24). Report to the ASTER GDEM Validation Team.

Tahirkheli, R. A. K., Mattauer, N., Proust, F., & Tapponier, P. (1979). The India–Eurasia suture zone in northern Pakistan: Synthesis and interpretation of recent data at plate scale. In A. Farah & K. A. De Jong (Eds.), *Geodynamics of Pakistan* (pp. 125–130). Quetta: Geological Survey of Pakistan.

Walsh, L. S., Martin, A. J., Ojha, T. P., & Fedenczuk, T. (2012). Correlations of fluvial knickzones with landslide dams, lithologic contacts, and faults in the southwestern Annapurna Range, central Nepalese Himalaya. *Journal of Geophysical Research, 117,* 1–24.

Whipple, K. X. (2004). Bedrock rivers and the geomorphology of active orogens. *Annual Review of Earth and Planetary Sciences, 32,* 151–185.

Whipple, K. X., Hancock, G. S., & Anderson, R. S. (2000). River incision into bedrock: Mechanics and relative efficacy of plucking, abrasion, and cavitation. *Geological Society of America Bulletin, 112,* 490–503.

Whipple, K. X., & Tucker, G. E. (1999). Dynamics of the stream-power river incision model: Implications for height limits of mountain ranges, landscape response timescales, and research needs. *Journal of Geophysical Research, 104,* 17661–17674.

Wills, C. J., & McCrink, T. P. (2002). Comparing landslide inventories: The map depends on the method. *Environmental and Engineering Geoscience, 8,* 4279–4293.

Wobus, C., Whipple, K. X., Kirby, E., Snyder, N., Johnson, J., Spyropolou, K., Crosby, B., & Sheehan, D. (2006). *Tectonics form topography: Procedures, promise, and pitfalls* (pp. 55–74). GSA Special Paper 398, Penrose Conference Series.

Zeitler, P. K., Johnson, N. M., Waeser, G. W., & Tahirkheli, R. A. K. (1982). Fission-track evidence for Quaternary uplift of the Nanga Parbat region, Pakistan. *Nature, 298,* 255–257.